Optimal 8PSK mappings for BICM-ID over quasi-static fading channels

W. R. Carson and I. J. Wassell
Computer Laboratory
University of Cambridge
United Kingdom

M. R. D. Rodrigues
Instituto de Telecomunicações
Department of Computer Science
University of Porto, Portugal

***Abstract*—In this paper, we investigate the optimal mapping scheme for 8PSK for an iterative demapping and decoding system over quasi-static fading channels. We show that there are only 86 unique 8PSK mappings and conjecture that only 70 8PSK mappings will have unique error performance characteristics. We obtain an analytical expression for the demapper *extrinsic* information transfer (EXIT) functions using a Binary Erasure Channel (BEC) to model *a-priori* information and use this to help select the mapping that converges earliest to a bit error rate (BER) value of 10^{-5}. Finally, we present the performance of the optimal mapping scheme and compare its performance with mappings that have the lowest bit error floor, earliest convergence threshold and best non-iterative performance over an additive white Gaussian noise (AWGN) channel.**

I. INTRODUCTION

Turbo or iterative techniques have been proposed for a large number of communication scenarios including multi-user processing [1], space-time processing [2] and the processing of bit interleaved coded modulation with iterative decoding (BICM-ID) [3]. They have been shown to exhibit excellent performance over the AWGN channel [4].

The quasi-static fading channel is extremely important because it models various practical scenarios characterised by extremely low time and frequency diversity, e.g., fixed wireless access (FWA) channels. Iterative techniques have been shown to improve performance in these channels however it has been observed that the choice of mapping scheme can have a dramatic effect on system performance [5]. It is therefore important to match the encoder and mapper appropriately. For our system model, two or more mapping schemes may result in identical system performance, this implies that we need only consider a subsection of the $8! = 40,320$ mappings possible with 8PSK. Brännström and Rasmussen use a bit-wise distance criterion to classify all 8PSK mappings into 86 sub-sets [6].

This paper investigates the process of selecting an optimal 8PSK mapping scheme. Section II introduces the system model. Sections III, IV, V and VI demonstrate the existence of several equivalent mappings, leading to a reduction of the entire set of 8PSK mappings. In Section VI we also introduce the BEC approximation to the AWGN *a-priori* channel model for EXIT charts. Section VII provides the final BER simulation results and our optimal mapping. Finally, the main conclusions of this work are summarised in Section VIII.

II. SYSTEM MODEL

Fig.1 depicts the communications system model. We consider both single antenna systems ($N_T = N_R = 1$) often known as single-input single-output (SISO), which do not exploit space diversity, as well as multiple antenna systems ($N_T, N_R > 1$), which do exploit space diversity. The transmitter consists of four main stages: the encoder, the interleaver, the mapper and the space-time processor (see Fig.1). Initially, the information bits are convolutionally encoded at rate R_c, these coded bits are then pseudo-random interleaved. Finally, groups of 3 interleaved coded bits are mapped to a complex symbol from a unit power 8-ary phase shift keying (PSK) constellation.

In multiple transmit antenna systems ($N_T > 1$), the space-time processing block generates a space-time block code (STBC) according to the generator matrices $\mathbf{G}_2$, $\mathbf{G}_3$ or $\mathbf{G}_4$ given by [7]. Essentially, a total of $K \times N_T$ symbols obtained from the original K' modulation symbols are transmitted during K time slots by N_T transmit antennas.

The signal is distorted by a frequency-flat quasi-static fading channel as well as AWGN. Consequently, we express the relationship between the complex receive symbols and the complex transmit symbols associated with a specific STBC frame as:

$$\mathbf{r} = \mathbf{h}\mathbf{s} + \mathbf{n} \tag{1}$$

Here, $\mathbf{r}$ denotes the $N_R \times K$ matrix whose element $r_j(k)$ denotes the complex receive symbol at time slot k and receive antenna j; $\mathbf{s}$ denotes the $N_T \times K$ matrix whose element $s_i(k)$ denotes the complex transmit symbol at time slot k and transmit antenna i; $\mathbf{h}$ denotes the $N_R \times N_T$ matrix of channel gains whose element $h_{j,i}$ denotes the channel gain from transmit antenna i to receive antenna j (note that $h_{j,i}$ is independent of time slot k); and $\mathbf{n}$ denotes the $N_R \times K$ matrix whose element $n_j(k)$ denotes the noise random variable at time slot k and receive antenna j. The channel gains are uncorrelated circularly symmetric complex Gaussian with mean zero and variance $\frac{1}{2}$ per dimension. The noise random variables are uncorrelated circularly symmetric complex Gaussian with mean zero and variance $\frac{1}{2 \cdot SNR_{norm}} = \frac{N_T}{2 \cdot SNR}$ per dimension, where SNR denotes the average signal-to-noise ratio per receive antenna.

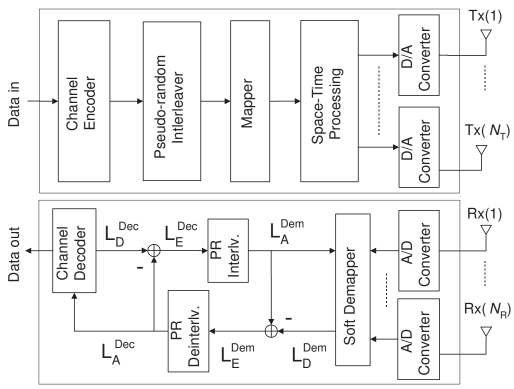

Fig. 1: Communications system model.

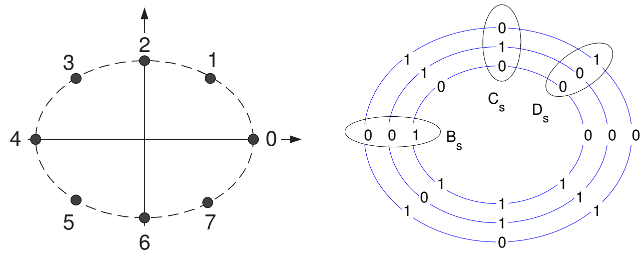

(a) Octal mapping (b) Binary sub-mapping

Fig. 2: Two possible representations of Natural mapping

The receiver consists of two main parts: (i) the soft demapper and (ii) the soft-in soft-out decoder. These two stages are separated by pseudo-random interleavers and de-interleavers, and they exchange soft information in an iterative manner (see Fig.1). Specifically, the soft demapper takes as *a priori* information L_A^{Dem} on the code bits which is an interleaved version of the *extrinsic* information L_E^{Dec} on the code bits produced by the soft input-soft output decoder. Then, it computes the *a-posteriori* information L_D^{Dem} of the code bits, a log-likelihood ratio (LLR) from which we remove L_A^{Dem} to give L_E^{Dem}, the *extrinsic* information. The *extrinsic* information is then used as the *a-priori* input for the log-MAP algorithm [8] decoder, and is given by:

$$L_E^{Dem}(b_m(k)|\mathbf{r}) = ln \frac{\sum\limits_{(\mathbf{s}\in\mathbf{s}^+)} p(\mathbf{r}|\mathbf{s}) \prod\limits_{\substack{m'=1\\ m'\neq m}}^{log_2 M} \prod\limits_{\substack{k'=1\\ k'\neq k}}^{K'} Pr(b_{m'}(k'))}{\sum\limits_{(\mathbf{s}\in\mathbf{s}^-)} p(\mathbf{r}|\mathbf{s}) \prod\limits_{\substack{m'=1\\ m'\neq m}}^{log_2 M} \prod\limits_{\substack{k'=1\\ k'\neq k}}^{K'} Pr(b_{m'}(k'))} \quad (2)$$

where $b_m(k)$ is the m^{th} bit conveyed by the k^{th} mapped symbol, $\mathbf{s}^+ = \{\mathbf{s}\text{: } b_m(k)=1\}$), and $\mathbf{s}^- = \{\mathbf{s}\text{: } b_m(k)=0\}$).

The eight positions in an 8PSK constellation are described by $S(q) = \sqrt{E_s}e^{j\frac{2\pi q}{8}}$ for $q = 0, 1, ..., 7$. The average symbol energy is given by $E_s = 3R_cE_b$ where E_b is the average energy per information bit. The 3-bit symbols are mapped to the constellation positions using a mapping l, such that the symbol at $S(q)$ is given by $l(q)$; the elements of l are expressed in octal notation. For example, the mapping in Fig. 2(a) is given by $l_1 = [0, 1, 2, 3, 4, 5, 6, 7]$ and is known as natural mapping. A mapping is divided into three sub-mappings, each of which maps one of the bits in the 3-bit symbols to the constellation positions. We assign the following labels to the three sub-mappings (B, C, D), the three Hamming weight one 8PSK symbols (B_s, C_s, D_s) and the three Hamming weight two 8PSK symbols $(\overline{B_s}, \overline{C_s}, \overline{D_s})$.

There is a special relationship between these symbols and these sub-mappings: the single weight of symbol A_s is contained in sub-mapping A, furthermore $\overline{A_s}$ is the logical complement of the bit sequence of symbol A_s, for $A \in \{B, C, D\}$. Therefore we are only able to assign one of these sets of labels freely since this will define the other two sets. There are therefore $3! = 6$ possible distinct labellings for each mapping.

Consider natural mapping, its three sub-mappings correspond to the three rings in Fig. 2(b). We choose the following labelling scheme for these sub-mappings:

$$l_1 = BCD = \begin{bmatrix} 000 \\ 001 \\ 010 \\ 011 \\ 100 \\ 101 \\ 110 \\ 111 \end{bmatrix} = \begin{bmatrix} 00001111 \\ 00110011 \\ 01010101 \end{bmatrix}' \quad (3)$$

where $'$ denotes the transpose operator. The first sub-mapping label in l_1 is assigned to the inner most sub-mapping, the second label to the central sub-mapping and the final label to the outer most sub-mapping. Therefore for our choice of natural sub-mapping labels we get: $B_s = 100$, $C_s = 010$, $D_s = 001$ and $\overline{B_s} = 011$, $\overline{C_s} = 101$, $\overline{D_s} = 110$.

III. Mapping Operators

When considering the mapping choice for our system model, we introduce four operators that take advantage of our assumptions on the channel noise and input bit distribution to drastically reduce the number of unique 8PSK mappings. The first two operators maintain the relative order of the symbols, using the assumption of circularly symmetric noise, to identify equivalent mappings. The next two operators maintain the Hamming distance between the constellation positions, using the assumption of equi-probable symbols at the channel input, to identify equivalent mappings. These final two operators have also been presented in [9] as the interchanging and complementation of rows (sub-mappings) respectively. If the mappings are viewed as a number expressed in octal, then we are able to index them in ascending order (See [6]), e.g. $l_1 = [0, 1, 2, 3, 4, 5, 6, 7]$ and $l_{40320} = [7, 6, 5, 4, 3, 2, 1, 0]$. We illustrate the effect of the operators on natural mapping (l_1).

A. Constellation Rotation (Cr): $l_{5914} = [1, 2, 3, 4, 5, 6, 7, 0]$

Under the assumption of circularly symmetric noise, rotating the constellation positions of the symbols will not affect performance, i.e., all mappings $l(q) = S(q + t)$ for $t \in \mathbb{Z}$ are equivalent, e.g., $l_1 \equiv l_{5914}$. We refer to this operation of rotation as Constellation Rotation (Cr). The Cr operation gives a set expansion of eight, i.e., it gives a total of eight different mappings that are equivalent.

B. Constellation Reflection (Cf): $l_{5040} = [0, 7, 6, 5, 4, 3, 2, 1]$

Under the assumption of circularly symmetric noise, reflecting the constellation positions of the symbols will not affect performance, i.e., both mappings $l(q) = S(tq)$ for $t = \pm 1$ are equivalent, e.g., $l_1 \equiv l_{5040}$. We refer to this type of operation accordingly as constellation reflection (Cf). The Cf operation gives a set expansion of two.

C. Sub-mapping Reordering (Sr): $l_{289} = \begin{bmatrix} 00110011 \\ 00001111 \\ 01010101 \end{bmatrix}'$

Under the assumption of equi-probable input symbols, reordering the sub-mappings will not affect performance, e.g., $l_1 \equiv l_{289}$. We obtained l_{289} by exchanging sub-mappings B and C, $l_{289} = CBD$. We note that this reordering has affected the symbol labels, we now have $B_s = 010$, $C_s = 100$ and $D_s = 001$. We refer to this type of operation as sub-mapping reordering (Sr). The Sr operation gives a set expansion of $3! = 6$.

D. Bit Flipping (Bf): $l_{23617} = \begin{bmatrix} 11110000 \\ 00110011 \\ 01010101 \end{bmatrix}'$

Under the assumption of equi-probable symbols, complementation of one of the sub-mappings will not affect performance, e.g., $l_1 \equiv l_{23617}$. This operation can also be represented by the exclusive OR operation with symbol X, where $X \in \{B_s, C_s, D_s, \overline{B_s}, \overline{C_s}, \overline{D_s}, 111\}$. We obtained l_{2355} by the complementation of sub-mapping B or $X = B_s$. We note that the bit flipping operation does not affect the symbol values, i.e., $B_s = 100$, $C_s = 010$ and $D_s = 001$. The Bf operation gives a set expansion of $2^3 = 8$.

IV. Set reducing operator combinations

Using these four operators a mapping may generate a full set expansion of 768. Unfortunately, for some mappings combinations of the operators will generate the original mapping, they will therefore not have a full set expansion. Consider $l_1 = [0, 1, 2, 3, 4, 5, 6, 7]$, if we Bf with $X = B_s$ we generate $l_{23617} = [4, 5, 6, 7, 0, 1, 2, 3]$ and we observe that with a simple Cr operation we can return to the original mapping, l_1. Therefore l_1 will not have a full set expansion.

We found that there are twelve combinations of operators that could render the original mapping, called T_1 to T_{12}. These combinations were deduced by careful consideration of the effect that operators have on the phase relationships in a mapping. We introduce the following notation for Table I: the combination of mapping operators is denoted by the concatenation of their abbreviations, e.g., CrBf, and the phase of symbol S_2 anti-clockwise from S_1 is denoted by $\theta(S_1, S_2)$. Some phase relationships are used repeatedly, so we abbreviate them further: $\alpha = \theta(000, 111)$, $\beta = \theta(B_s, \overline{B_s})$, $\kappa = \theta(C_s, \overline{C_s})$ and $\delta = \theta(D_s, \overline{D_s})$. Each operator combination has particular phase requirements a mapping must satisfy, Table I.

T_1	CrBf $X = B_s$	$\alpha = \beta \neq \pi$ $\kappa = -\delta \neq \pi$	$\theta(000, B_s) = \pi$ $\theta(C_s, \overline{D_s}) = \pi$
T_2	CrBf $X = \overline{B_s}$	$\alpha = -\beta \neq \pi$ $\kappa = \delta \neq \pi$	$\theta(000, \overline{B_s}) = \pi$ $\theta(C_s, D_s) = \pi$
T_3	CrBf $X = 111$	$\alpha = \beta = \kappa = \delta = \pi$	
T_4	CrCfBf $X = B_s$	$\alpha = -\beta$ $\kappa = \delta$	$\theta(000, B_s)$ is odd $\theta(000, C_s) = \theta(\overline{D_s}, B_s)$
T_5	CrCfBf $X = \overline{B_s}$	$\alpha = \beta$ $\kappa = -\delta$	$\theta(000, \overline{B_s})$ is odd $\theta(000, C_s) = \theta(D_s, \overline{B_s})$
T_6	CrCfBf $X = 111$		$\theta(000, 111)$ is odd $\theta(000, B_s) = \theta(\overline{B_s}, 111)$
T_7	CrSrBf $X = B_s, l_c = CBD$	$\alpha = \beta = \kappa = -\delta \neq \pi$	$\theta(000, B_s) = \pm\frac{\pi}{2}$ $\theta(000, \overline{D_s}) = \pi$ $\theta(000, C_s) = \mp\frac{\pi}{2}$
T_8	CrSrBf $X = \overline{B_s}, l_c = CBD$	$-\alpha = \beta = \kappa = \delta \neq \pi$	$\theta(000, \overline{B_s}) = \pm\frac{\pi}{2}$ $\theta(000, \overline{D_s}) = \pi$ $\theta(000, \overline{C_s}) = \mp\frac{\pi}{2}$
T_9	CrSrBf $X = B_s, l_c = BDC$	$\alpha = \beta \neq \pi$ $\kappa = \delta = \pi$	$\theta(000, B_s) = \pi$
T_{10}	CrSrBf $X = 111, l_c = BDC$	$\alpha = \beta = \pi$ $\kappa = -\delta \neq \pi$	$\theta(C_s, \overline{D_s}) = \pi$
T_{11}	CrSrCfBf $X = B_s, l_c = BDC$	$\alpha = -\beta$	$\theta(000, B_s)$ is odd $\theta(000, C_s) = \theta(\overline{C_s}, B_s)$
T_{12}	CrSrCfBf $X = 111, l_c = BDC$	$\kappa = \delta$	$\theta(000, 111)$ is odd $\theta(000, B_s) = \theta(\overline{B_s}, 111)$ $\theta(000, C_s) = \theta(\overline{D_s}, 111)$

TABLE I: Table of all set reducing operator combinations.

The labelling scheme that we choose to apply to a mapping will not affect which combinations it satisfies, however in Table I we have chosen a labelling that focuses on symbols B_s or $\overline{B_s}$. Therefore when considering whether or not a mapping satisfies a particular combination, we should choose labellings that will also focus on symbols B_s and $\overline{B_s}$. If we are unable to find such a labelling scheme then the mapping will not satisfy the operator combination. For example, it is apparent that l_1 satisfies T_1 if we set $B_s = 100, C_s = 010, D_s = 001$. However because $\theta(000, 100) = \pi$ for l_1 we will be unable to satisfy T_2 since phase requirement $\theta(000, \overline{B_s}) = \pi$ is always violated regardless of our values of B_s, C_s, D_s.

A single mapping generates an entire set expansion and we have calculated that there are a total of 86 non-equivalent non-overlapping set expansions in 8PSK. We deduced that there are 56 sets with reduced set expansions and calculated the size of these sets. Therefore we can calculate that there are 30 non-equivalent sets with full set expansions. We divide these 86 unique sub-sets of 8PSK into 15 groups according to the combinations they satisfy and label them accordingly, Table II. The table details the operator combinations a sub-set satisfies and its size (A_c).

A sub-set is generated from a mapping by using the four mapping operators, however the operators affect the phase

Mapping Name	Multiple combinations		A_c	
L0 - L29			768	
M1a - d	T_1 T_4 (T_5)		192	
M2a - b	T_1 T_6 (T_5)		192	
M3a - b	T_2 T_4 T_8 (T_{11} T_{12})		96	
M4a	T_2 T_4		192	
M5a - b	T_2 T_5 T_7 (T_{11} T_{12})		96	
M6a	T_2 T_5		192	
M7a - b	T_2 T_6 (T_4)		192	
M8a - b	T_3 T_4 (T_5)		192	
M9a - f	T_4		384	
M10a - d	T_5		384	
M11a - b	T_6		384	
N1a - d	T_9 T_5 (T_{12})	T_{10} T_5 (T_{11})	96	96
N2a - d	T_9	T_{10}	192	192
N3a - t	T_{11}	T_{12}	192	192

TABLE II: Table showing the 15 groupings of operator combinations

relationships of a mapping and some Bf operations can generate a mapping with phase relationships that satisfy different operator combinations to the original mapping. For the first 12 sub-set groupings in Table II the mappings in a set expansion all satisfy the same combinations, but for the final three groups the mappings in the set expansions will satisfy one of two collections of operator combinations. We present both in the Multiple combinations column, and the number of mappings that satisfy each collection in a set expansion. The size of set expansion of a mapping and the number of operator combinations it satisfies are related. The set expansion will halve for each non-parenthesised combination it satisfies. The combinations in parenthesis are satisfied coincidentally, they are the result of the non-parenthesised combinations and the phase restrictions these combinations place on a mapping, hence they do not contribute to the set reduction.

V. Bit-wise Distance Spectra

We are able to gain further insight into the unique 8PSK mappings by considering their bit-wise distance spectrum [6]. The bit-wise distance spectra with zero *a-priori* information for any mapping is defined below and is denoted by W_0; here and in the rest of the paper we use the sub-index b to represent the number of known bits

$$W_0 \triangleq \begin{bmatrix} w_0^1(1) & w_0^1(2) & w_0^1(3) & w_0^1(4) \\ w_0^2(1) & w_0^2(2) & w_0^2(3) & w_0^2(4) \\ w_0^3(1) & w_0^3(2) & w_0^3(3) & w_0^3(4) \end{bmatrix}, \quad (4)$$

where $w_0^i(j)$ denotes the average of the total Hamming distance for bit position $i = 1, 2...m$ of a symbol to all other symbols at Euclidean distance d_j, for all symbols. We calculate this term below, where the Hamming distance between i^{th} bits of the symbols at S_n and S_m is $d_H(S_n^i, S_m^i)$.

$$w_0^i(j = 1, 2, 3) = \frac{1}{4} \sum_{n=0}^{7} d_H(S_n^i, S_{n+j}^i), \quad (5)$$

$$w_0^i(j = 4) = \frac{1}{8} \sum_{n=0}^{7} d_H(S_n^i, S_{n+4}^i). \quad (6)$$

The elements of bit-wise distance spectrum for full *a-priori* information are defined in a similar fashion, except that symbols are considered if they only differ in the i^{th} bit.

We introduce the notation $I_{E,b}$ to represent the average demapper Mutual information when b bits are known. It was reasoned in [6] that the *extrinsic* Mutual information for zero *a-priori* information, $I_{E,0}$, is dependent on W_0, we would further conjecture that it is a function of the sum of the bit-wise distance spectra, $w_0(j) \triangleq \sum_{i=1}^{m} w_0^i(j)$. Similarly, it has been proved in [6] that the *extrinsic* Mutual Information for full *a-priori* information, $I_{E,2}$, is a function of the sum of the bit-wise distance spectra, $w_2(j)$:

$$I_{E,2} = \frac{1}{m} \sum_{j=1}^{M/2} w_2(j) J \left[\sqrt{8\gamma_s} sin\left(\frac{\pi j}{M}\right) \right]. \quad (7)$$

Using this classification, we can see from (5) and (6) that the mapping operators will not affect the values of w_0 or w_2, and hence equivalent mappings will have the same $[w_0, w_2]$ values. Furthermore, we have found that there are only 70 unique pairings of $[w_0, w_2]$, implying that some non-equivalent mappings have equivalent $[w_0, w_2]$ values. We therefore evaluated how these special non-equivalent mappings performed, through EXIT charts and BER plots.

Finally, we present all 86 unique sub-sets in table III. We give the sub-set name, set expansion size (A_c), the mapping with the lowest index in the sub-set (l_c), its mapping index (c) and sub-set distance spectra values $[w_0, w_2]$. Some mappings are already well known and we also include these names: Gray, Natural (N), Set partitioning (SP) [10], modified set partitioning (MSP), semi-set partitioning (SSP) [11], and Maximum squared Euclidean weight (MSEW) [10].

VI. EXIT Charts

For a similar BICM-ID system over a quasi-static fading channel it was shown that the convergence threshold dictates error performance [12]. For an iteratively decoded system a standard tool for predicting the convergence threshold has been ten Brink's EXIT charts [13]. Therefore although we are able to classify mappings for zero and full *a-priori* information, we are particularly interested in the form of the EXIT curve in the region between these two points.

There are three main methods to model the *a-priori* information in an iterative system [14]:

- Model it as an AWGN channel. This is ten Brink's assumption for EXIT charts.
- Model it as a BEC with erasure probability ϵ.
- Model it as a BSC with cross-over probability p.

We propose to approximate the AWGN *a-priori* channel with a BEC channel with erasure probability ϵ. We are then able to derive the EXIT chart function (the *extrinsic* mutual information I_E) as a quadratic in terms of the *a-priori* mutual information I_A. We make use of the well-known relationship between the mutual information and erasure probability of the BEC, $I = 1 - \epsilon$

$$I_E(I_A) = (1 - I_A)^2 I_{E,0} + I_A(1 - I_A) I_{E,1} + (I_A)^2 I_{E,2}. \quad (8)$$

It was further shown by ten Brink that for independent and uniformly distributed binary inputs the area under this EXIT

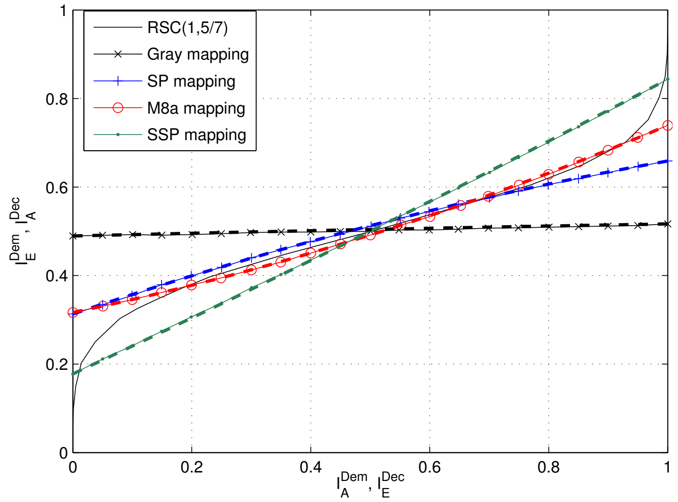

Fig. 3: EXIT charts for various 8PSK mappings for an $E_b/N_0 = 6.1$dB. Solid line correspond to AWGN *a-priori* information, dashed lines to BEC *a-priori* information.

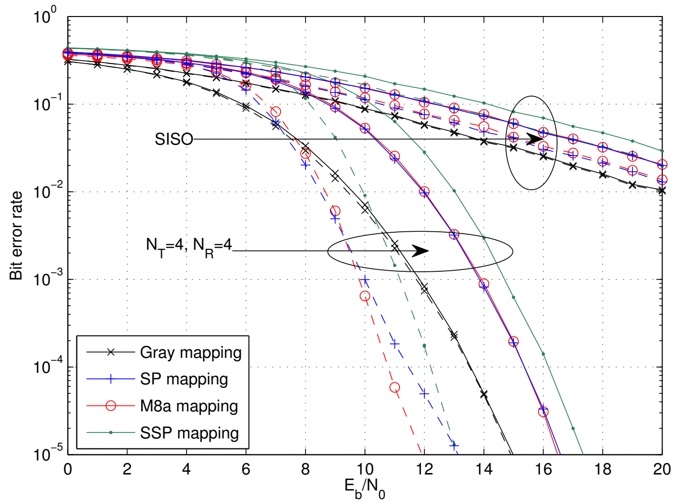

Fig. 4: BER versus E_b/N_0 performance curves for 8PSK mappings over various quasi-static channel settings. Solid lines 1 iteration, dashed lines 8 iterations.

chart curve is equal to the capacity of the constellation, this is known as the area property. The capacity of a constellation is independent of the mappings scheme implemented, therefore we can rewrite the demapper EXIT function as a function of only two mapping dependent terms, $I_{E,0}$ and $I_{E,2}$, and the constellation constrained capacity, C_{8PSK}:

$$\begin{aligned} I_E(I_A) &= [3(I_{E,2} + I_{E,0}) - 2C_{8PSK}](I_A)^2 \\ &\quad +[2C_{8PSK} - 2I_{E,2} - 4I_{E,0}]I_A + I_{E,0}. \end{aligned} \tag{9}$$

We have found that using the BEC as an approximation to the AWGN *a-priori* channel provides tight approximation for the EXIT chart curve of the demapper. We considered a wide range of E_b/N_0 and mapping schemes, Fig. 3. Using this model, we make a further conjecture that non-equivalent mappings with equivalent $[w_0, w_2]$ values will have the same error performance characteristics. Therefore we need only consider 70 non-equivalent 8PSK sub-sets.

Using the BEC *a-priori* approximation we are able to draw some guidelines for mapping selection for a particular convolutional code. Consider that at the convergence threshold of a turbo code, the decoding trajectory is able to just squeeze past the bottleneck between the two decoding EXIT functions and traverse the whole EXIT chart to the top right corner. This leads to a sudden sharp decrease in the BER curve. In order to achieve similar performance for our system we would also require the first intersection of the demapper and decoder EXIT curves at the convergence threshold to be as close to $I_A^{Dem} = 1$ as possible; this is more likely with concave, rather that convex, functions. For example, consider the SP mapping, Fig. 3; due to its convexity it intersects with the decoder EXIT curve earlier than would be desired. For this mapping there is a more gradual transition from a high to low BER at the convergence threshold.

The quadratic coefficient of (9) can be used to measure the concavity/convexity of EXIT functions. Furthermore due to the area property, for a fixed $I_{E,0}$ the lower the value of $I_{E,2}$ the greater the degree of convexity, but the higher the bit error rate. We define early convergence to a BER value of 10^{-5} as our optimisation criterion. There is therefore a trade-off between early convergence and low error floors.

VII. Simulation Results

This section investigates the performance of iterative demapping and decoding techniques over frequency-flat quasi-static fading channels both with and without antenna diversity. We considered the 86 unique 8PSK mapping schemes coupled with a rate $1/2$ RSC code with octal generator polynomial $(1, 5/7)$. We will emphasise differences in performance in the quasi-static fading and the AWGN regimes for BER performance curves. In our simulations, we consider a frame length of 2052 and a soft input-soft output decoder implementing the log-MAP algorithm.

We propose the mapping M8a ($c = 48$) as optimal for our system model, the performance curves in Fig. 4 illustrate its performance both with and without antenna diversity. We compare its performance with three other mapping schemes: Gray mapping, which has been shown to have the best BER performance for non-iterative systems; semi-set partitioning (SSP) mapping, which has the lowest bit error floor for 8PSK; set partitioning (SP) mapping, which has a convex EXIT function and has the lowest convergence threshold. It is actually difficult to ascertain that SP mapping has the lowest convergence threshold from EXIT charts, and indeed there are a few mappings with very similar thresholds.

The EXIT functions for these four mappings are depicted in Fig. 3, as well as each BEC approximation curve and the decoder EXIT function. We observe that the M8a EXIT function has a high initial value and a slightly concave EXIT function, this combination enables it to have a much sharper BER plot decrease than SP mapping while having a much earlier convergence than SSP mapping.

We observe that iterating increases the performance in all scenarios with the exception of Gray mapping, which does not benefit. Both SP and M8a mappings have identical performance in systems with limited antenna diversity, and both outperform SSP mapping over all scenarios (antennas, iterations) over all E_b/N_0. For systems with significant antenna diversity for low E_b/N_0 SP mapping outperforms M8a mapping, however this corresponds to high BER values. We observe that M8a mapping outperforms the other three mappings for systems with significant antenna diversity at medium to high E_b/N_0 by approximately 1dB.

VIII. Conclusions

We observed that we can classify all 8PSK mappings into 86 sub-sets under comprehensive assumptions, with all mappings within a sub-set being equivalent. Furthermore we conjecture that only 70 of these sub-sets will have unique error performance characteristics. We show that using the BEC as an approximation to the AWGN for the *a-priori* channel in EXIT charts gives very good results and enables a quadratic description of the EXIT curve. We use this analytical description to help aid our selection of an optimal mapping for our system model, M8a mapping, and compare its BER performance with mappings that are also optimal for different criteria. Results demonstrate that M8a mapping outperforms other mappings for our system with high antenna diversity and medium to high E_b/N_0. For systems that are non-iterative or have low antenna diversity, we observed that Gray mapping outperforms all other mappings for all E_b/N_0.

Acknowledgement

The authors would especially like to thank Dr. Ioannis Chatzigeorgiou for valuable discussions and comments.

References

[1] X. Wang and H. V. Poor, "Iterative (turbo) soft interference cancellation and decoding for coded CDMA," in *IEEE Trans. Commun.*, vol. 47, July 1999, pp. 1046–1061.

[2] B. Lu and X. Wang, "Iterative receivers for multiuser space-time coding systems," in *IEEE J. Select. Areas Commun.*, vol. 18, Nov. 2000, pp. 2322–2335.

[3] S. ten Brink, J. Speidel, and R. H. Yan, "Iterative demapping and decoding for multilevel modulation," in *Proc. IEEE Globecom '98*, vol. 1, July 1998, pp. 579–584.

[4] C. Berrou and A. Glavieux, "Near optimum error correcting coding and decoding: Turbo codes," in *IEEE Trans. Commun.*, vol. 44, Oct. 1996, pp. 1261–1271.

[5] W. R. Carson, I. Chatzigerorgiou, M. R. D. Rodrigues, I. J. Wassell, and R. Carrasco, "On the performance of iterative demapping and decoding techniques over quasi-static fading channels," in *Proc. PIMRC 2007*, Sept. 2007.

[6] F. Brännström and L. K. Rasmussen, "Classification of 8PSK mappings for BICM," in *Proc. IEEE ISIT '07*, June 2007, pp. 2136–2140.

[7] V. Tarokh, H. Jafarkhani, and A. R. Calderbank, "Space-time block coding for wireless communications: Performance results," in *IEEE J. Select. Areas Commun.*, vol. 17, Mar. 1999, pp. 451–460.

[8] P. Robertson, E. Villebrun, and P. Höeher, "A comparison of optimal and sub-optimal MAP decoding algorithms operating in the log domain," in *Proc. IEEE ICC '95*, June 1995, pp. 1009–1013.

[9] C. Stierstorfer and R. F. Fischer, "(Gray) mappings for bit-interleaved coded modulation," in *Proc. IEEE VTC '07*, Apr. 2007, pp. 1703–1707.

[10] J. Tan and G. L. Stüber, "Analysis and design of symbol mappers for iteratively decoded BICM," in *IEEE Trans. Wireless Commun.*, Mar. 2005, pp. 662–672.

[11] X. Li, A. Chindapol, and J. A. Ritcey, "Bit-interleaved coded modulation with iterative decoding and 8PSK signaling," in *IEEE Trans. Commun.*, Aug. 2002, pp. 1250–1257.

[12] W. R. Carson, M. R. D. Rodrigues, and I. J. Wassell, "Modelling the frame error rate for iterative dempaping and decoding techniques over a quasi-static fading channel," in *Proc. IEEE Sarnoff '08*, Apr. 2008.

[13] S. ten Brink, "Convergence behaviour of iteratively decoded parallel concatenated codes," in *IEEE Trans. Commun.*, vol. 49, no. 10, Oct. 2001, pp. 1727–1737.

[14] J. Hagenauer, "EXIT CHART - Introduction to extrinsic information transfet in iterative processing," in *Proc. EUSIPICO '04*, Sept. 2004.

c	Name	A_c	l_c	w_0	w_2
138	M3a, Gray	12	0,1,3,2,6,7,5,4	2.00 4.00 4.00 2.00	2.00 0.00 1.00 0.00
24	M3b	24	0,1,2,3,7,6,5,4	2.50 3.00 3.50 3.00	1.50 1.00 0.50 0.00
18	N3v	48	0,1,2,3,6,7,5,4	2.50 3.00 4.00 2.50	1.50 1.00 0.50 0.00
22	N1d	24	0,1,2,3,7,5,6,4	2.50 3.00 4.50 2.00	1.50 1.00 0.00 0.50
12	L0	96	0,1,2,3,5,7,6,4	2.50 3.50 4.00 2.00	1.50 0.75 0.50 0.25
92	N2d	48	0,1,2,6,7,3,5,4	2.50 4.00 3.50 2.00	1.50 0.50 0.50 0.50
132	N3j	48	0,1,3,2,5,7,6,4		1.75 0.00 1.25 0.00
82	M9d	48	0,1,2,6,4,5,7,3	2.50 4.00 4.00 1.50	1.50 0.50 0.50 0.50
122	M1c	24	0,1,3,2,4,5,7,6	2.50 5.00 3.50 1.00	1.50 0.00 0.50 1.00
17	M5b	12	0,1,2,3,6,7,4,5	3.00 2.00 5.00 2.00	1.00 2.00 0.00 0.00
42	M9f	48	0,1,2,4,6,7,5,3	3.00 3.00 3.50 2.50	1.00 1.00 1.00 0.00
16	L1	96	0,1,2,3,6,5,7,4	3.00 3.00 4.00 2.00	1.00 1.25 0.50 0.25
11	M10d	48	0,1,2,3,5,7,4,6		1.00 1.50 0.50 0.00
41	N3a	48	0,1,2,4,6,7,3,5	3.00 3.00 4.50 1.50	1.00 1.00 0.50 0.50
54	N3r	48	0,1,2,5,3,7,6,4		1.25 1.00 0.25 0.50
10	L2	96	0,1,2,3,5,6,7,4	3.00 3.50 3.00 2.00	1.00 1.00 1.00 0.00
36	L3	96	0,1,2,4,5,7,6,3	3.00 3.50 3.50 2.00	1.00 0.75 1.00 0.25
4	L4	96	0,1,2,3,4,6,7,5		1.25 0.75 0.75 0.25
58	L5	96	0,1,2,5,4,6,7,3		
38	L6	96	0,1,2,4,6,3,7,5	3.00 3.50 4.00 1.50	1.00 1.00 0.50 0.50
68	L7	96	0,1,2,5,7,3,6,4		1.25 0.75 0.25 0.75
8	M6a	24	0,1,2,3,5,4,7,6	3.00 4.00 3.00 2.00	1.00 1.00 1.00 0.00
88	M4a	24	0,1,2,6,5,4,7,3		
127	M7b	24	0,1,3,2,5,4,6,7		1.50 0.00 1.50 0.00
35	L8	96	0,1,2,4,5,7,3,6	3.00 4.00 3.50 1.50	1.00 0.50 1.00 0.50
112	M9a	48	0,1,2,7,5,4,6,3		
2	L9	96	0,1,2,3,4,5,7,6		1.25 0.50 0.75 0.50
80	N3o	48	0,1,2,6,4,3,7,5		
89	N3n	48	0,1,2,6,5,7,3,4		
81	N3p	48	0,1,2,6,4,5,3,7	3.00 4.00 4.00 1.00	1.25 0.50 0.25 1.00
32	L10	96	0,1,2,4,5,3,7,6	3.00 4.50 3.00 1.50	1.00 0.50 1.00 0.50
6	L11	96	0,1,2,3,4,7,6,5	3.50 2.50 4.50 1.50	0.75 1.50 0.25 0.50
48	M8a	24	0,1,2,4,7,6,5,3	3.50 3.00 2.50 3.00	0.50 1.00 1.50 0.00
72	M9e	48	0,1,2,5,7,6,4,3	3.50 3.00 3.00 2.50	1.00 1.00 1.00 0.00
46	N2b	48	0,1,2,4,7,5,6,3	3.50 3.00 3.50 2.00	0.50 1.00 1.00 0.50
47	N1b	24	0,1,2,4,7,6,3,5		
5	L12	96	0,1,2,3,4,7,5,6		0.75 1.25 0.75 0.25
28	L13	96	0,1,2,4,3,6,7,5		
64	N3f	48	0,1,2,5,6,4,7,3		0.75 1.50 0.75 0.00
53	N3g	48	0,1,2,5,3,7,4,6		
3	N1c	24	0,1,2,3,4,6,5,7		1.00 1.00 0.50 0.50
71	N2a	48	0,1,2,5,7,6,3,4		
30	L14	96	0,1,2,4,3,7,6,5	3.50 3.00 4.00 1.50	0.75 1.00 0.75 0.50
39	N3i	48	0,1,2,4,6,5,3,7		
65	M11a	48	0,1,2,5,6,7,3,4		1.00 1.00 0.50 0.50
106	M1a, MSP	24	0,1,2,7,4,5,6,3	3.50 3.00 4.50 1.00	0.50 1.00 0.50 1.00
1	M2b, N, SP	24	0,1,2,3,4,5,6,7		1.00 1.00 0.00 1.00
29	L15	96	0,1,2,4,3,7,5,6	3.50 3.50 3.00 2.00	0.75 0.75 1.25 0.25
33	L16	96	0,1,2,4,5,6,3,7		
67	L17	96	0,1,2,5,7,3,4,6		1.00 0.75 1.00 0.25
44	L18	96	0,1,2,4,7,3,6,5	3.50 3.50 3.50 1.50	0.50 0.75 1.00 0.75
26	L19	96	0,1,2,4,3,5,7,6		0.75 1.00 0.75 0.50
59	L20	96	0,1,2,5,4,7,3,6		
57	L21	96	0,1,2,5,4,6,3,7		1.00 0.75 0.50 0.75
43	N2c	48	0,1,2,4,7,3,5,6	3.50 4.00 2.50 2.00	0.50 0.50 1.50 0.50
151	N3c	48	0,1,3,4,5,2,6,7		1.25 0.00 1.75 0.00
31	N3e	48	0,1,2,4,5,3,6,7	3.50 4.00 3.00 1.50	0.75 0.50 1.25 0.50
111	L22	96	0,1,2,7,5,4,3,6		
206	N3h	48	0,1,3,6,5,2,7,4		
56	L23	96	0,1,2,5,4,3,7,6		1.00 0.50 1.00 0.50
87	M9c	48	0,1,2,6,5,4,3,7		
105	M10b	48	0,1,2,7,4,5,3,6	3.50 4.00 3.50 1.00	0.50 0.50 1.00 1.00
146	M10a	48	0,1,3,4,2,5,7,6		1.00 0.50 0.50 1.00
609	M1d	24	0,1,7,2,4,5,3,6	3.50 5.00 2.50 1.00	0.50 0.00 1.50 1.00
66	M7a	24	0,1,2,5,6,7,4,3	4.00 2.00 4.00 2.00	0.50 2.00 0.50 0.00
27	N3t	48	0,1,2,4,3,6,5,7	4.00 3.00 2.50 2.50	0.50 1.00 1.50 0.00
51	L24	96	0,1,2,5,3,6,4,7	4.00 3.00 3.00 2.00	0.50 1.25 1.00 0.25
50	M10c	48	0,1,2,5,3,4,7,6		0.50 1.50 1.00 0.00
25	M11b	48	0,1,2,4,3,5,6,7	4.00 3.00 3.50 1.50	0.50 1.00 1.00 0.50
49	L25	96	0,1,2,5,3,4,6,7		0.75 1.00 0.75 0.50
63	N3k	48	0,1,2,5,6,4,3,7		
104	N3q	48	0,1,2,7,4,3,6,5	4.00 3.00 4.00 1.00	0.25 1.00 0.75 1.00
55	N3l	48	0,1,2,5,4,3,6,7		0.75 1.00 0.25 1.00
163	L26	96	0,1,3,4,7,2,5,6	4.00 3.50 2.50 2.00	0.50 0.75 1.50 0.25
103	L27	96	0,1,2,7,4,3,5,6	4.00 3.50 3.00 1.50	0.25 0.75 1.25 0.75
85	L28	96	0,1,2,6,5,3,4,7		0.50 1.00 1.00 0.50
495	M3b	12	0,1,6,2,5,4,3,7	4.00 4.00 2.00 2.00	1.00 0.00 2.00 0.00
519	M9b	48	0,1,6,3,5,4,2,7	4.00 4.00 2.50 1.50	0.50 0.50 1.50 0.50
607	N3m	48	0,1,7,2,4,3,5,6	4.00 4.00 3.00 1.00	0.25 0.50 1.25 1.00
61	L29	96	0,1,2,5,6,3,4,7	4.50 2.50 3.50 1.50	0.25 1.50 0.75 0.50
1699	N1a, MSEW	24	0,3,4,1,7,2,5,6	4.50 3.00 2.50 2.00	0.00 1.00 1.50 0.50
517	N3d	48	0,1,6,3,5,2,4,7	4.50 3.00 3.00 1.50	0.25 1.00 1.25 0.50
493	N3b	48	0,1,6,2,5,3,4,7		0.50 1.00 1.00 0.50
1777	M2a, SSP, MSEW	24	0,3,4,7,1,2,5,6	4.50 3.00 3.50 1.00	0.00 1.00 1.00 1.00
513	M1b	24	0,1,6,3,4,5,2,7		0.50 1.00 0.50 1.00
1695	M5a, MSEW	12	0,3,4,1,6,5,2,7	5.00 2.00 3.00 2.00	0.00 2.00 1.00 0.00

TABLE III: Table of 8PSK sub-sets